Polyhedron 39 (2012) 1–8

Contents lists available at SciVerse ScienceDirect

Polyhedron

journal homepage: www.elsevier.com/locate/poly

New dimeric and supramolecular mixed ligand Palladium(II) dithiocarbamates as potent DNA binders

Hizbullah Khan [a,b], Amin Badshah [a,*], Zia-ur- Rehman [a], Muhammad Said [a], Ghulam Murtaza [a], Afzal Shah [a], Ian S. Butler [b], Safeer Ahmed [a], Frédéric-Georges Fontaine [c]

[a] Department of Chemistry, Quaid-I-Azam University, Islamabad 45320, Pakistan
[b] Department of Chemistry, McGill University, 801 Sherbrooke St., W. Montreal, Quebec, Canada H3A 2K6
[c] Département de Chimie, Université Laval, 1045 Avenue de la Médecine, Québec, Canada G1V 0A6

ARTICLE INFO

Article history:
Received 29 November 2011
Accepted 13 February 2012
Available online 1 March 2012

Keywords:
DNA binding study
Palladium
Mixed ligand
Dithiocarbamate

ABSTRACT

Five Pd(II)-based potential potent metallopharmaceuticals (**1**–**5**) of the general formula [(DT)Pd(PR_3)Cl], where DT = dibutyldithiocarbamate (**1**,**2**), dipropyldithiocarbamate (**3**), bis(2-methoxyethyl)-dithiocarbamate (**4**), dimethyldithiocarbamate (**5**); PR_3 = triphenylphosphine (**1**), diphenyl-*p*-tolylphosphine (**2**), diphenyl-*t*-butylphosphine (**3**), diphenyl-2-methoxyphenylphosphine (**4**), *p*-cholorodiphenylphosphine (**5**), have been synthesized and characterized using FT-IR, Raman, and multinuclear-NMR spectroscopy. The X-ray single crystal analysis (**1** and **2**) reveals the Pd(II) moiety is in a distorted square–planar arrangement with two positions being occupied by the bidentate dithiocarbamate ligand, while the other two positions are occupied by a phosphine ligand and a chloro group. The packing diagrams confirmed that the intermolecular Cl···H interactions are not only the main cause of deviation from an ideal square planar geometry, but are also responsible for the Pd–S bond lengths variation. The DNA binding ability of the complexes was examined by cyclic voltammetry (CV). The cyclic voltammograms of the synthesized metallopharmaceuticals followed irreversible electrochemical behavior, which indicate the high reactivity of the reduced form of complexes. The results obtained from CV evidenced the catalytic role of DNA in enhancing the electron transfer processes of the complexes. The DNA binding studies are expected to provide useful insights about the unexplored mechanism by which anticancer drugs exert their biochemical action.

1. Introduction

Cisplatin is an important anticancer drug, but it suffers from acquired resistance, neuro-, nephro-, oto-, gastrointestinal and bone marrow toxicity [1]. In the previous two decades, there has been a continuous interest in the synthesis of more potent drug complexes containing S- and N-donor ligands that should have higher cytotoxic activity with minimum or no side effects as compared to cisplatin [2]. After extensive experimental screening, Das and Livingstone postulated that sulfur containing palladium(II) complexes are more effective anticancer drugs [3]. The aminothiol (NH_2–$(CH_2)_3$–NH–$(CH_2)_2$–S–PO_3H_2) was found to protect against chemo and radiotherapy side-effects, potentially because of the release of the tridentate N, N, S aminothiol [4]. In combined therapy, glutathione has also shown an evident reduction in the nephrotoxicity of cisplatin and carboplatin [5]. It has been reported that thiols and glutathione bind to the $(NH_3)Pt^+$ moiety, causing ammonia release [6]. Thiocarbonyl donors have also demonstrated chemoprotectant properties in modulating the nephrotoxicity of cisplatin [7].

Cleare and Hoeshele suggested some prominent structure/activity rules: *trans*-compounds, charged ones and those having only one leaving group are inactive while complexes having two amine ligands with at least one H atom are active [8]. However, some complexes, like *trans*-[$PtCl_2$(L)(L′)] with L and/or L′ = pyridine-like ligands, L = alkyl substituted amine and L′ = isopropyl amine, and L and/or L′ = iminoether, violate these criteria [9].

Dithiocarbamates have shown promising results in reversing the renal cellular damage caused by cisplatin in several animal models [10]. These ligands selectively remove the platinum metal from the enzyme-thiol complex without reducing the antitumor effect of the drug [11a]. Trevisan and co-workers found Pd(II) dithiocarbamates to have anticancer activity like cisplatin with the additional advantage of no cross-resistance [11a,b].

Keeping in view the objective of synthesizing palladium complexes having maximal antitumor activity and little toxic side effects when compared to cisplatin, we synthesized and

* Corresponding author. Tel.: +92 051 90642131; fax: +92 05190642241.
E-mail addresses: aminbadshah@yahoo.com (A. Badshah), frederic.fontaine@chm.ulaval.ca (F.-G. Fontaine).

0277-5387/$ - see front matter © 2012 Elsevier Ltd. All rights reserved.
doi:10.1016/j.poly.2012.02.025

characterized mixed ligand palladium(II) complexes of the general formula [(DT)Pd(II)(PR_3)Cl] (DT = dibutyldithiocarbamate, dipropyldithiocarbamate, bis(2-methoxyethyl) dithiocarbamate or dimethyldithiocarbamate; PR_3 = triphenylphosphine, diphenyl-p-tolylphosphine, diphenyl-t-butylphosphine, diphenyl-2-methoxyphenylphosphine, or p-cholorodiphenylphosphine). Moreover, the DNA binding ability of the palladium drugs were investigated by cyclic voltammetry (CV) with the objective of adding effective chemotherapeutic agents to the arsenal of weapons used against cancer.

2. Results and discussion

2.1. Synthesis of the dithiocarbamate palladium(II) complexes and their characterization in solution

Complexes **1**–**5** were synthesized by reacting the appropriate dithiocarbamic acid and $(PR_3)_2PdCl_2$ in CH_2Cl_2 (Scheme 1). The complexes are soluble in common organic solvents and are stable under normal conditions of temperature and pressure.

In addition to the absorption bands associated with the phosphine ligands, complexes **1**–**5** display IR stretching modes at ν_{max} values of 1512–1530 (CN), 995–1096 (SCS_{asym}), 701–689 (SCS_{sym}) and 380–388 cm^{-1} (Pd-S), suggesting coordination of the dithiocarbamate ligand to the metal. The diagnostic band in the 1450–1580 cm^{-1} range is attributable to the C–N stretching mode and is highly characteristic of dithiocarbamate complexes [12]. This C–N vibration appears at a value between that normally found for a single bond (1250–1350 cm^{-1}) and a double bond (1640–1690 cm^{-1}). This intermediate bond length was also confirmed using X-ray crystallography (*vide infra*) [13], suggesting that the resonance structure I is dominant compared to the others (Scheme 2) and that the C–N bond strength is increased compared to that of the free ligand [14]. The absence of an S–H absorption band in the 2550–2700 cm^{-1} region indicates that in all cases replacement of the hydrogen atom of the SH group by a metal ion has occurred. The appearance of a single absorption band for the SCS moiety in the 900–1100 cm^{-1} (SCS_{asym}) region and one in the 680–705 cm^{-1} region (SCS_{sym}) shows the complete symmetrically bonded nature of the dithiocarbamate ligand in a bidentate fashion [15].

The ^1H NMR data show the disappearance of the SH frequency, once more suggesting coordination of the dithiocarbamate moiety to the metal center by abstraction of H^+ from the dithiocarbamic acid. Another characteristic feature of the ^1H NMR spectra is the asymmetry in the alkyl groups attached to the nitrogen atom of the dithiocarbamate moiety, caused by the restricted rotation around the CN bond which is known to have an energy barrier of 65–92 kJ mol^{-1} [16]. The SCS carbon shift appeared in the range 206.2–208.5 ppm in the ^{13}C NMR spectra of the complexes. A slight decrease in the chemical shift of the SCS carbon atom compared to dithiocarbamic acid suggests complexation of the ligand to the palladium center. Similarly to the features observed by ^1H NMR spectroscopy, the carbon atoms of the substituents of the dithiocarbamate moiety are non-equivalent.

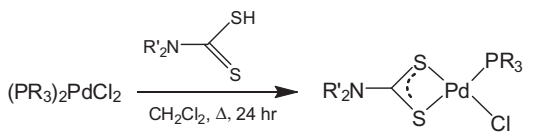

PR_3 = PPh_3 (**1**), PPh_2(*p*-tolyl) (**2**), PPh_2(*t*Bu) (**3**), PPh_2(*o*-OMe-Ph) (**4**), PPh_2Cl (**5**)

R' = butyl (**1**, **2**), propyl (**3**), 2-methoxyethyl (**4**), methyl (**5**)

Scheme 1. Synthesis of the mixed ligand Pd(II) complexes.

2.2. Structural study of complexes *1* and *2*

The molecular structures and selected distances and angles of compounds **1** and **2** are shown in Figs. 1 and 3, respectively. Complex **1** crystallizes in the triclinic crystal system ($P\bar{1}$), whereas **2** crystallizes in the $P2_1/c$ monoclinic system. Both complexes exhibit a similar pseudo square-planar geometry, with the S atoms of the dithiocarbamate ligand occupying two adjacent coordination sites and with the chloride and the phosphine binding to the two remaining sites. The largest distortion from the normal geometry comes from the bidentate ligand (S(1)–Pd(1)–S(2) of 75.41(3) and 75.48(2)° for **1** and **2**, respectively), which causes the *trans* S(2)–Pd(1)–Cl(1) and P(1)–Pd(1)–S(1) angles to be between 167.75(3) and 171.53(2)°, smaller than the expected value of 180°. The increase in the *trans* S–Pd–Cl angle can also be attributed to the involvement of the chloro group in intermolecular non-covalent interactions. The high *trans* angle of **2** compared to **1** is possibly due to stronger Cl···H intermolecular interactions (Figs. 2 and 4) in **2** (2.830 Å) than **1** (2.849 Å). Moreover, this also confirms the idea that the intermolecular Cl···H interaction is a main cause of the deviation of the square planar geometry from its ideal value. The dissymmetry observed in the Pd–S distances is typical for square-planar systems and reflects the *trans* influence of the ligands in play. In both complexes, the Pd(1)–S(1) bond lengths *trans* to the phosphine ligand are longer (2.3302(7) and 2.3566(5) Å for **1** and **2**, respectively) than the Pd(1)–S(2) bond lengths *trans* to the chloride (2.2966(7) and 2.2793(6) Å for **1** and **2**, respectively). The largest discrepancy in the Pd–S bond lengths for complex **2** (**ΔPd–S** of 0.077 Å for **2** compared to 0.034 Å for **1**) reflects the better donating capability of the PPh_2-*p*-tolyl ligand compared to triphenylphosphine. In addition to this, packing diagrams (Figs. 3 and 5) show stronger Cl···H intermolecular interactions in **2** (2.830 Å) compared to **1** (2.849 Å), and as a consequence the Pd–Cl bond is longer in **2** (2.3277 Å) than **1** (2.3226 Å). This allows the S atom *trans* to the chloro group to approach comparatively closely and to undergo a strong interaction with the Pd atom, thus causing the higher discrepancy in the Pd–S bond lengths in **2**. The S–C distances in **1** and **2** of 1.711(3) and 1.732(3) Å, respectively, are intermediate between normal C–S (1.82 Å) and C=S (1.60 Å) distances. Similarly, the C(1)–N(1) bond lengths of 1.312(3) Å for **1** and 1.318(3) Å for **2** are significantly shorter than a normal C–N bond (1.47 Å) and longer than a C=N bond (1.28 Å) [17]. These bond values clearly demonstrate the resonance phenomenon in the SCS moiety, as reported in the previous section.

The packing diagrams (Figs. 2 and 4) attribute a supramolecular ladder structure to complex 1, mediated by Bu–H···Cl and Ph–H···Cl intermolecular interactions, whereas complex 2 exhibits a dimeric structure due to the presence of intermolecular Cl···H interactions.

3. Cyclic voltammetry (CV)

3.1. Electrochemical characterization and DNA binding studies

The synthesized compounds were screened for their anticancer activity by a cyclic voltammetric based assay. Although easy to implement, this assay cannot be applied to electro-inactive compounds. Moreover, the method is limited to compounds exerting their anticancer effect through a direct interaction with DNA. In spite of these obvious limitations, this technique can differentiate the binding strength and modes of action of DNA-binding compounds.

Electrochemical studies of the synthesized Pd(II)-based potential anticancer compounds (**1**–**5**) were carried out with the objective of getting insight into their redox behaviour and DNA binding modes.

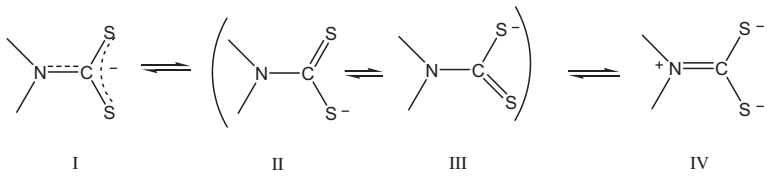

Scheme 2. Resonance structures of the dithiocarbamate moiety.

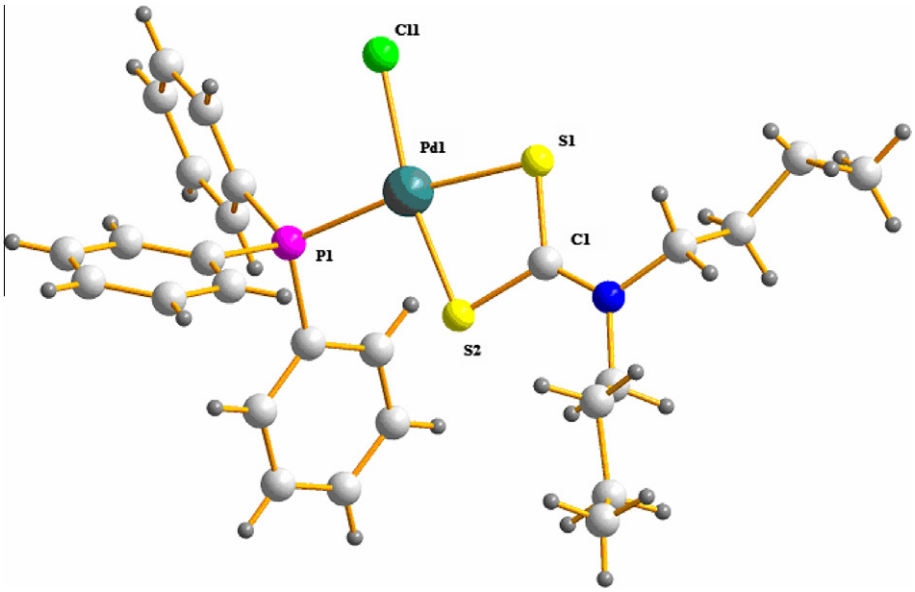

Fig. 1. Ball and stick representation of complex **1**. Selected bond lengths (Å) and angles (°): Pd(1)–P(1) 2.2926(7); Pd(1)–Cl(1) 2.3226(7); Pd(1)–S(1) 2.3302(7); Pd(1)–S(2) 2.2966(7); S(1)–C(1) 1.711(3); S(2)–C(1) 1.732(3); C(1)–N(1) 1.312(3); P(1)–Pd(1)–Cl(1) 96.47(3); P(1)–Pd(1)–S(2) 95.63(3); S(2)–Pd(1)–S(1) 75.41(3); Cl(1)–Pd(1)–S(1) 92.58(3); S(2)–Pd(1)–Cl(1) 167.75(3); P(1)–Pd(1)–S(1) 170.64(2); C(1)–N(1)–C(2) 119.7(3); C(1)–N(1)–C(6) 122.2(2); C(6)–N(1)–C(2) 118.2(2); S(1)–C(1)–S(2) 110.57(15).

Typical cyclic voltammograms of the synthesized complexes **1** and **3** are depicted in Fig. 5. The relevant electrochemical parameters are assembled in Table 1.

The cyclic voltammograms of all five complexes registered a single broad cathodic peak corresponding to irreversible reduction of the analyte. The absence of a peak in the reverse scan indicates the instability of the reduced form of the complexes. The relatively difficult reduction of compounds **1**–**4**, as evident from their cathodic peaks at more negative potentials, can be linked to the low electron affinity of the electrophore due to the more nucleophilic nature of the electron-donating phosphine and dithiocarbamate attached to the metal. The reduction potential of the complexes followed the expected tendency of Tolman's electronic parameter (ν, cm^{-1}) of phosphines (PPh_2-*t*Bu < PPh_2-*p*-tolyl < PPh_3 < PPh_2Cl) [18]. The facile electro-reduction of compound **5** (Table 1) can be attributed to the presence of a strongly electron-withdrawing chloro group at the phosphine moiety. The peak current data of complex **5** was not so strong as to allow the calculation of the diffusion coefficient, $D°$, and heterogeneous rate constant, k_{sh}. The rationale behind the comparatively low peak current of complex **5** may be its interaction with the solvent due to the presence of an additional chloro group. The small hump at −1.14 and −1.15 V, noticed in the CV of complexes **1** and **2**, before the appearance of a prominent reduction peak can be related to inner sphere (within the complex molecule) and outer sphere (due to the solvent effect) rearrangements of the complexes, as reported previously for organometallic complexes [19].

The dependence of the current function I_p on the scan rate, ν, is an important diagnostic criterion for establishing the type of mechanism. For achieving this objective, the CVs of the complexes were recorded at various scan rates. The corresponding data of the complexes are listed in Table 1. The effect of scan rate on complex **3** is shown in Fig. 6. The shift in peak potential with the increase in scan rate manifests the irreversibility of the reduction process. However, the emergence of an oxidation hump at higher scan rates points to quasi-reversible behavior. The relatively large $D°$ values also suggest quasi-reversible kinetics [20]. The values of k_{sh} are of the magnitude expected for intermediate kinetic processes [21].

For the evaluation of the interaction parameters of Pd-based complexes with DNA, cyclic voltammetric measurements were performed, keeping the concentration of the complex constant (5 mM) and varying the concentration of DNA from 10 to 200 nM. Typical CVs of samples 1 and 3 with and without DNA are presented in Fig. 7. For both complexes, the reduction peak increased in height accompanied by a slight shift in the peak potential upon incremental addition of DNA. A dramatic change in the voltammetric response of complexes **1** and **3** was encountered in the presence of 35–50 nM DNA, when the reduction peak leveled off and another cathodic peak emerged exactly at the potential value of the small hump observed in the CV of the pure complexes. A literature survey regarding drug-DNA binding in solution has revealed three modes of interaction: (i) a decrease in peak current with no shift in peak potential value, ascribed to the consumption of the drug by DNA [22], (ii) a negative shift rationalized as electrostatic interactions between the anionic phosphate of DNA and the cationic moiety of the drug [23], and (iii) a positive shift related to the intercalation of the drug into the stacked base pairs of DNA [24]. The present novel situation (i.e., peak current enhancement of the complexes in the presence of DNA) can be attributed to the catalytic role of DNA in inducing an electron transfer to the

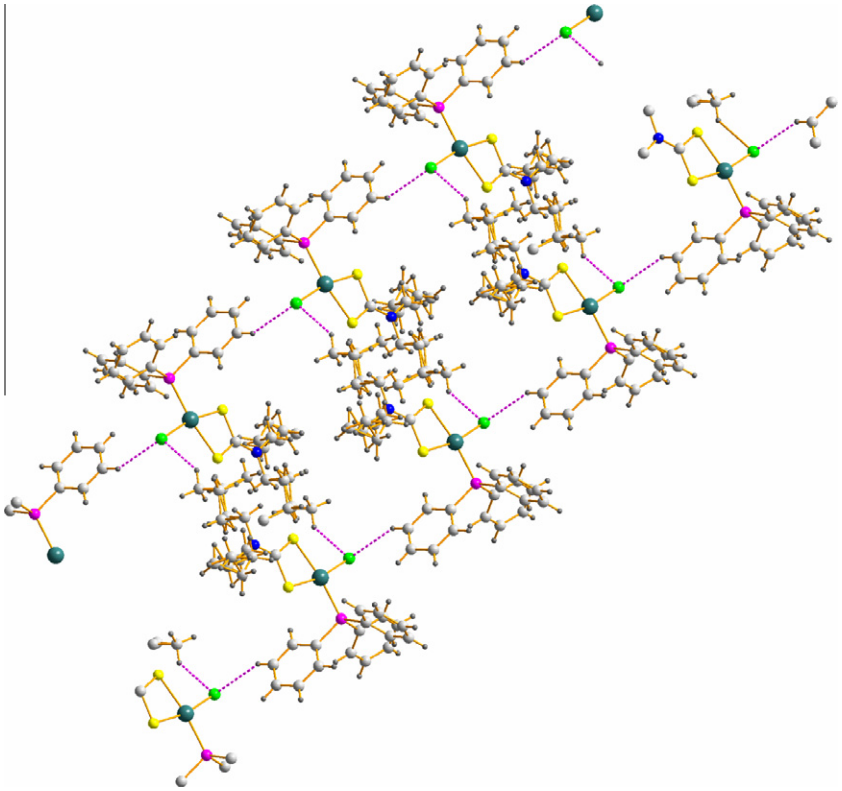

Fig. 2. Supramolecular chain structure of compound **1** mediated by Bu–H···Cl and Ph–H···Cl intermolecular interactions of 2.787 and 2.849 Å, respectively.

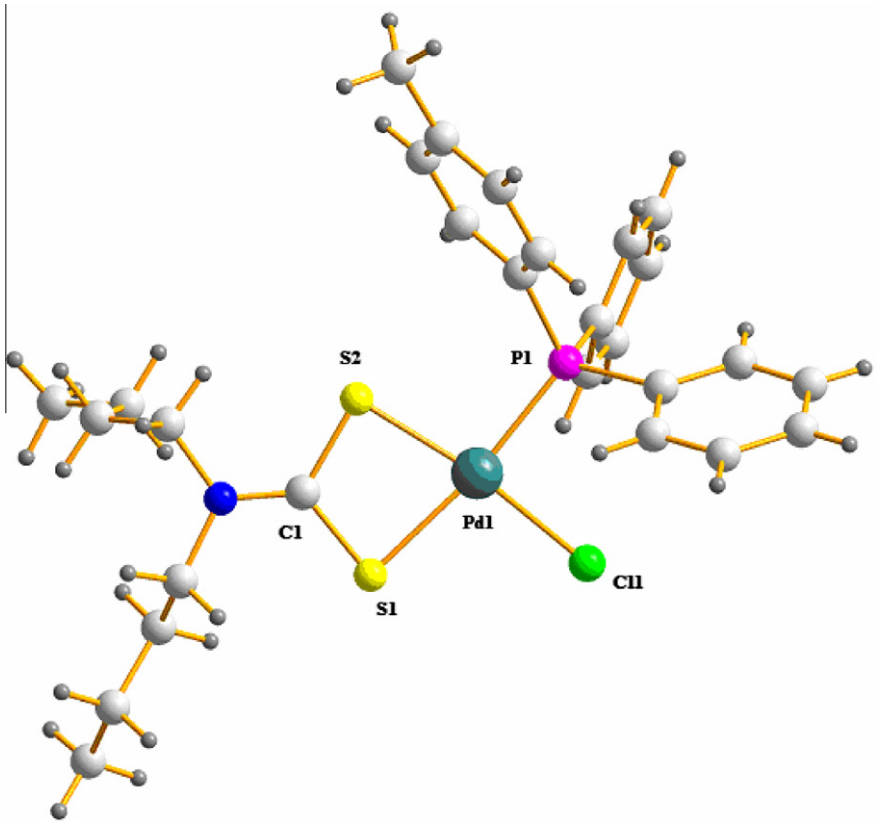

Fig. 3. Ball and stick representation of complex **2**. Hydrogen atoms have been omitted for clarity. Selected bond lengths (Å) and angles (°): Pd(1)–P(1) 2.2699(5); Pd(1)–Cl(1) 2.3277(6); Pd(1)–S(1) 2.3566(5); Pd(1)–S(2) 2.2793(6); S(1)–C(1) 1.717(2); S(2)–C(1) 1.731(2); C(1)–N(1) 1.318(3); P(1)–Pd(1)–Cl(1) 91.48(2); P(1)–Pd(1)–S(2) 96.412(19); S(2)–Pd(1)–S(1) 75.48(2); Cl(1)–Pd(1)–S(1) 96.81(2); S(2)–Pd(1)–Cl(1) 170.80(2); P(1)–Pd(1)–S(1) 171.53(2); C(1)–N(1)–C(2) 121.25(19); C(1)–N(1)–C(6) 120.70(19); C(6)–N(1)–C(2) 117.16(19); S(1)–C(1)–S(2) 110.79(12).

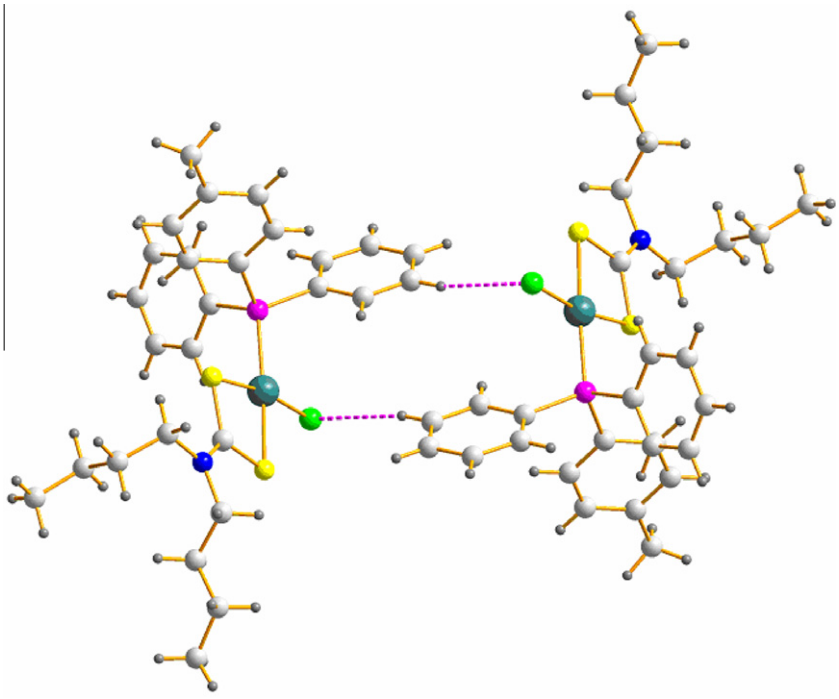

Fig. 4. Dimeric structure of compound **2** mediated by Cl···H interactions (2.830 Å).

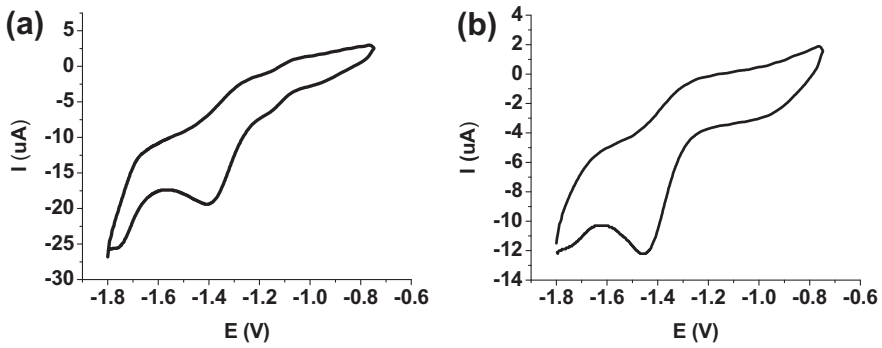

Fig. 5. Representative cyclic voltammograms of a 5 mM concentration of (A) 1 and (B) 3 in dichloromethane with a 0.1 M concentration of MTBAP at 25 °C on a glass carbon electrode vs. SCE at a 0.150 Vs^{-1} scan rate.

Table 1
Voltammetric and kinetic parameters of the complexes in dichloromethane at 25 °C on GC vs. SCE.

Substrate	E_{pc} (V)	I_{pc} (μA)	$E^c_p - E^c_{p/2}$ (V)	D° × 10^5 (cm^2/s)	k_{sh} × 10^4 (cm/s)
1	−1.387	17.79	0.076	5.1	5.8
2	−1.412	11.58	0.056	4.9	4.7
3	−1.463	9.87	0.044	4.3	4.6
4	−1.331	11.27	0.042	4.3	6.9
5	−0.899	1.08	0.130	–	–

Pd(II) complex. The increase in peak current intensity with the generation of no new peak has also been assigned to catalytic behavior by previous electrochemists [25]. An examination of the packing diagrams demonstrates that the chloro groups may be involved in hydrogen bonding with DNA bases in the same fashion as depicted in Figs. 2 and 4. Consequently, the electronic density in the vicinity of Pd will be lowered, which may lead to the enhancement of the electron transfer process, as evidenced from the increase in peak current intensity. The argument is further supported by the presence of two chloro groups in complex **5**, which has the highest DNA-binding affinity (Table 2). The lowest binding constant of complex **4** can be attributed to the presence of the more polar methoxy groups having a lower affinity for the DNA less polar interior. The high DNA-binding affinity of complex **1** may be due to the more hydrophobic butyl groups. The leveling off of the major reduction peak points to the unavailability of the free drug, resulting in the culmination of the catalytic effect of DNA.

From the data listed in Table 2, it can be inferred that the *K* values are of the order of 10^6 for compounds **1**, 2 and **5**, while the *K*

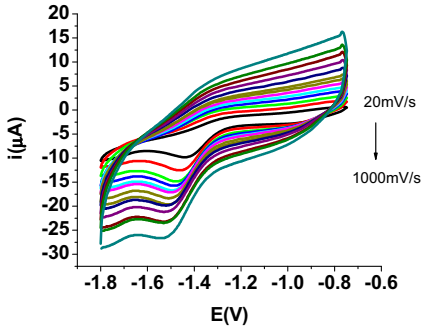

Fig. 6. Cyclic voltammograms of complex **3** (5 mM) in dichloromethane + 0.1MTBAP at 25 °C on GC vs. SCE at different scan rates.

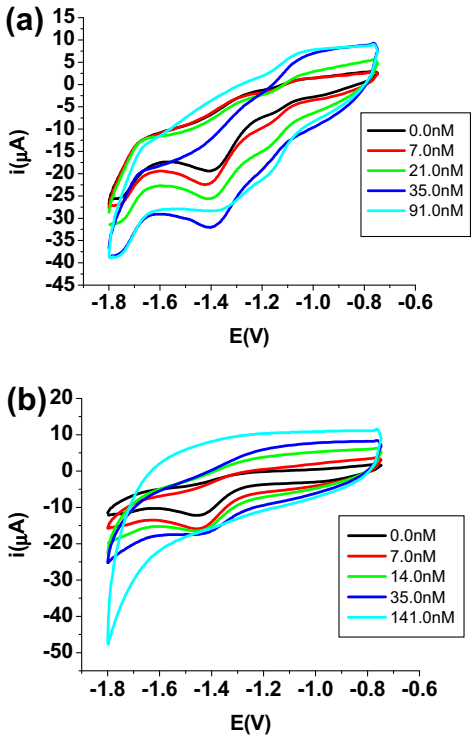

Fig. 7. Cyclic voltammograms depicting the effect of DNA concentration on the complexes (a) sample 1 (b) sample 3 at a constant (5 mM) concentration in dichloromethane + 0.1 M TBAP at 25 °C on GC vs. SCE at 0.150 Vs^{-1} scan rate.

Table 2
Binding parameters for the compounds based upon cyclic voltammetric data.

Substrate	K (M^{-1})	$-\Delta G^{\circ}$ (kJmol^{-1})
1	7.05×10^6	39
2	1.35×10^6	35
3	8.46×10^4	28
4	6.16×10^2	16
5	7.05×10^6	39

values of **3** and **4** are of the order of 10^4 and 10^2. The binding constants of these complexes are higher than those normally reported for drug molecules, i.e., 10^2–10^4 [26]. The DNA-binding affinity of complexes **1**, 2 and **5** are greater than $K = 4.1 \times 10^5\ M^{-1}$ for the clinically used anticancer drug epirubicin [27]. The high ΔG° values of complexes **1** and **5** ensure greater conformational stability of their DNA adducts.

4. Conclusions

Five new palladium(II) dithiocarbamates have been successfully synthesized and characterized by various analytical techniques. The X-ray single crystal structures of compounds **1** and **2** show that these species are pseudo square-planar with the dithiocarbamate ligands bonding in a *cis* fashion and with the Pd–S bond *trans* to the phosphine being longer than the Pd–S bond *trans* to the chloride. The involvement of the chloro group in secondary interactions not only plays a key role in this deviation (see the packing diagrams) but also has a marked influence on the DNA binding ability of complexes. The cyclic voltammograms of complexes **1**–**4** exhibit a single irreversible scan rate dependent reduction peak at −1.33 to −1.46 V (versu SCE). In the presence of DNA, an increase in peak current accompanied with a small cathodic shift in reduction potential evidenced the catalytic role of DNA in enhancing the electron transfer process. At higher concentrations, the catalytic effect of DNA was culminated. The negative ΔG° values indicate the spontaneity of the complexes-DNA binding. The binding constants varied in the sequence: $K_1 = K_5 > K_2 > K_3 > K_4$. The values of K for complexes **1**, 2 and **5** are greater than most of the clinically used anticancer drugs and these complexes may emerge as a new class of anticancer drugs after further investigations.

5. Experimental

5.1. General comments

All the experiments were performed under the normal conditions of temperature and pressure. Dimethylamine, *p*-chlorodiphenylphosphine, dibutylamine, triphenylphosphine, diphenyl-*p*-tolylphosphine, dipropylamine, diphenyl-*t*-butylphosphine, bis(2-methoxyethyl)amine, HCl, CS_2 and palladium(II) chloride were purchased from Aldrich Chemical Co. and were used without further purification. All the solvents were purified by the standard methods, dried, saturated with nitrogen and stored over molecular sieves (4 Å). NMR spectra were recorded on a Bruker 300 MHz spectrometer. ^{1}H NMR (300.13 MHz): $CDCl_3$ (7.26 ppm from $SiMe_4$) and DMSO-d_6 (2.49 ppm from $SiMe_4$), internal standard $SiMe_4$; ^{13}C NMR (75.46 MHz): internal standard TMS; the splitting of proton resonances in the NMR spectra are shown as: s = singlet, d = doublet, t = triplet and m = multiplet (showing a complex pattern). IR spectra were recorded on a Perkin–Elmer system 2000 FT-IR spectrometer (250–4000 cm^{-1}). The elemental analyses were conducted on a LECO-183 CHNS analyzer.

An Autolab PGSTAT 302 with software GPES (version 4.9, Eco Chemie, Utrecht, Netherland) was used to perform the cyclic voltammetry measurements. A standard calomel electrode was used as the reference electrode, a thin Pt-wire as a counter electrode and a bare glassy carbon (GC) electrode of 0.071 cm^2 area as a working electrode for all the measurements. All the measurements were carried out in CH_2Cl_2 (99.5%, Riedel-de Haen) using 0.1 M *t*-butyl ammonium perchlorate (TBAP ⩾ 98%, Fluka) at 25 ± 1 °C under an argon atmosphere. The sample concentration was maintained at 5 mM in each case.

5.2. General synthesis of complexes *1*–*5*

The palladium(II) phosphine complexes were prepared by dissolving the appropriate amount of Pd(II) chloride in methanol in the presence of 3 or 4 drops of concentrated HCl and by refluxing the solution for 30 min. The desired phosphine was dissolved in acetone and the solution was added to the Pd(II) chloride solution in a 2:1 M ratio. The reaction mixture was stirred under reflux for 3 h. The solid product obtained was filtered off and dried at room

temperature, dissolved in dichloromethane and reacted with the desired dithiocarbamate in a 1:1 M ratio. The reaction mixture was heated under reflux for 24 h. The resulting solution was decanted off and the solvent was removed under reduced pressure to form a golden yellow solid, which was dissolved in 30 mL of a mixture of dichloromethane, *n*-hexane and diethyl ether (2:1:1) and kept for recrystallization at room temperature in a 100 mL conical flask. Golden yellow crystals of 1 and 2 were obtained, but the other products were not crystalline under these conditions.

5.2.1. [Pd(dibutyldithiocarbamate)(PPh$_3$)Cl] (**1**)

Quantities used were 0.28 g (4.0 mmol) of dibutyldithiocarbamate and 2.80 g (4.0 mmol) Pd(PPh$_3$)$_2$Cl$_2$ in 25 mL of dichloromethane. Yield 80% (0.24 g) of golden yellow crystals. M.p. 171–172 °C. FT-IR (powder, cm^{-1}): 3072, 2925, 1526, 1093, 798, 691, 388, 320. ^{1}H NMR (300 MHz, CDCl$_3$) δ: 7.73–7.66 (m, 9H, Ar*H*), 7.47–7.40 (m, 6H, Ar*H*), 3.63 (t, 2H, –NC*H*$_2$, $^3J_{H-H}$ = 7.5 Hz), 3.48 (t, 2H, –NC*H*$_2$, $^3J_{H-H}$ = 7.5 Hz), 1.68–1.50 (m, 4H, –C*H*$_2$C*H*$_2$CH$_3$), 1.38–1.23 (m, 4H, -C*H*$_2$C*H*$_2$CH$_3$), 0.94 (t, 3H, –CH$_2$C*H*$_3$, $^3J_{H-H}$ = 7.2 Hz), 0.88 (t, 3H, –CH$_2$C*H*$_3$, $^3J_{H-H}$ = 7.2 Hz). ^{13}C{^{1}H} NMR (75.47 MHz, CDCl$_3$) δ: 206.2 (1C, –*C*SS), 134.5 (3C, Ar), 130.7 (6C, Ar), 128.8 (6C, Ar), 128.7 (3C, Ar), 48.9 (1C, –NCH$_2$), 48.8 (1C, –NCH$_2$), 29.1 (1C, –*C*H$_2$CH$_2$CH$_3$), 29.0 (1C, –*C*H$_2$CH$_2$CH$_3$), 20.0 (1C, –*C*H$_2$CH$_3$), 19.8 (1C, –*C*H$_2$CH$_3$), 13.7 (1C, –*C*H$_3$), 13.6 (1C, –*C*H$_3$). ^{31}P{^{1}H} NMR (121.49 MHz, CDCl$_3$) δ: 26.4. *Anal.* Calc. for C$_{27}$H$_{33}$ClNPPdS$_2$: C, 53.29; H, 5.47; N, 2.30; S, 10.54. Found: C, 53.31; H, 5.48; N, 2.33; S, 10.51%.

5.2.2. [Pd(dibutyldithiocarbamate)(PPh$_2$-*p*-tolyl)] (**2**)

Quantities used were 0.28 g (4.0 mmol) dibutyldithiocarbamate and 2.91 g (4.0 mmol) Pd(PPh$_2$-*o*-tolyl)$_2$Cl$_2$ in 25 mL of dichloromethane. Yield: 82% (0.28 g) of golden yellow crystals. M.p. 195–196 °C. FTIR (powder, cm^{-1}): 3049, 2930, 1512, 1433, 1095, 804, 747, 694, 380, 315. ^{1}H NMR (300 MHz, CDCl$_3$) δ: 7.74–7.58 (m, 8H, Ar*H*), 7.44–7.32 (m, 4H, Ar*H*), 7.28–7.19 (m, 2H, Ar*H*), 3.64 (t, 2H, –NC*H*$_2$, $^3J_{H-H}$ = 7.8 Hz), 3.49 (t, 2H, –NC*H*$_2$, $^3J_{H-H}$ = 7.8 Hz), 1.73 (s, 3H, –C*H*$_3$(*p*-tol)), 1.66–1.53 (m, 4H, –C*H*$_2$C*H*$_2$CH$_3$), 1.38–1.23 (m, 4H, –C*H*$_2$C*H*$_2$CH$_3$), 0.94 (t, 3H, –CH$_2$C*H*$_3$, $^3J_{H-H}$ = 7.5 Hz), 0.89 (t, 3H, –CH$_2$C*H*$_3$, $^3J_{H-H}$ = 7.2 Hz). ^{13}C{^{1}H} NMR (75.47 MHz, CDCl$_3$) δ: 206.3 (1C, –*C*SS), 137.3 (1C, Ar), 135.1 (9C, Ar), 134.0, 128.4 (8C, Ar), 49.0 (1C, –NCH$_2$), 48.8 (1C, –NCH$_2$), 29.2 (1C, –*C*H$_2$CH$_2$CH$_3$), 29.1 (1C, –*C*H$_2$CH$_2$CH$_3$), 20.0 (1C, –*C*H$_2$CH$_3$), 19.8 (1C, –*C*H$_2$CH$_3$), 13.7 (1C, –*C*H$_3$), 13.6 (1C, –*C*H$_3$). ^{31}P{^{1}H} NMR (121.49 MHz, CDCl$_3$) δ: 22.9. *Anal.* Calc. for C$_{28}$H$_{35}$ClNPPdS$_2$: C, 54.02; H, 5.67; N, 2.25; S, 10.30. Found: C, 54.08; H, 5.68; N, 2.27; S, 10.34%.

5.2.3. [Pd(dipropyldithiocarbamate)(PPh$_2$-*t*-butyl)Cl] (**3**)

Quantities used were 0.70 g (4.0 mmol) of dipropyldithiocarbamate and 2.65 g (4.0 mmol) of Pd(PPh$_2$-*t*-butyl)$_2$Cl$_2$ in dichloromethane. Yield: 85% (0.27 g) of a golden yellow solid. M.p. 155–156 °C. FTIR (powder, cm^{-1}): 3051, 2959, 1512, 1432, 1246, 1095, 742, 693, 382, 316. ^{1}H NMR (300 MHz, CDCl$_3$) δ: 7.50–7.46 (m, 6H, Ar*H*), 7.44–7.40 (m, 4H, Ar*H*), 3.93 (t, 2H, –NC*H*$_2$, $^3J_{H-H}$ = 7.5 Hz), 2.99 (t, 2H, –NC*H*$_2$, $^3J_{H-H}$ = 7.5 Hz), 1.88–1.77 (m, 2H, –C*H*$_2$CH$_3$), 1.74–1.66 (m, 2H, –C*H*$_2$CH$_3$), 1.00 (s, 9H, –C(C*H*$_3$)$_3$), 0.94 (t, 3H, –CH$_2$C*H*$_3$, $^3J_{H-H}$ = 7.5 Hz), 0.88 (t, 3H, –CH$_2$C*H*$_3$, $^3J_{H-H}$ = 7.5 Hz). ^{13}C{^{1}H} NMR (75.47 MHz, CDCl$_3$) δ: 206.5 (1C, –*C*SS), 134.9 (4C, Ar), 129.9 (2C, Ar), 127.6 (6C, Ar), 55.5 (1C, –NCH$_2$), 47.9 (1C, –NCH$_2$), 30.0 (1C, *C*(CH$_3$)$_3$), 27.8 (1C, C(CH$_3$)$_3$), 20.3 (1C, –C*H*$_2$CH$_3$), 19.0 (1C, –C*H*$_2$CH$_3$), 11.4 (1C, –*C*H$_3$), 11.3 (1C, –*C*H$_3$). ^{31}P{^{1}H} NMR (121.49 MHz, CDCl$_3$) δ: 46.9. *Anal.* Calc. for C$_{23}$H$_{33}$ClNPdS$_2$: C, 52.17; H, 6.28; N, 2.65; S, 12.11. Found: C, 52.12; H, 6.26; N, 2.64; S, 12.16%.

5.2.4. [Pd(bis(2-methoxyethyl)-dithiocarbamate)(PPh$_2$-*o*-OMe-Ph)Cl] (**4**)

Quantities used were 0.99 g (4.0 mmol) of bis(2-methoxyethyl)-dithiocarbamate and 3.04 g (4.0 mmol) Pd(PPh$_2$-o-tolyl)$_2$Cl$_2$ in 25 mL of dichloromethane. Yield: 90% (0.30 g) of a golden yellow solid. M.p. 175–176 °C. FTIR (powder, cm^{-1}): 3060, 2962, 1520, 1412, 1257, 995, 790, 701, 385, 322. ^{1}H NMR (300 MHz, CDCl$_3$) δ: 7.40–7.33 (m, 7H, Ar*H*), 7.32–7.25 (m, 6H, Ar*H*), 7.15 (t, 1H, Ar*H*, $^3J_{H-H}$ = 7.6 Hz), 3.72 (t, 2H, –CH$_2$C*H*$_2$, $^3J_{H-H}$ = 6.9 Hz), 3.70 (t, 2H, –CH$_2$C*H*$_2$, $^3J_{H-H}$ = 6.9 Hz), 3.30 (s, 6H, –CH$_2$OC*H*$_3$), 3.24 (t, 2H, –NC*H*$_2$, $^3J_{H-H}$ = 6.3 Hz), 3.22 (t, 2H, –NC*H*$_2$, $^3J_{H-H}$ = 6.3 Hz), 1.82 (s, 3H, Ar-OC*H*$_3$). ^{13}C{^{1}H} NMR (75.47 MHz, CDCl$_3$) δ: 206.2 (1C, -CSS), 159.8 (1C, Ar), 135.6 (2C, Ar), 134.2 (5C, Ar), 128.2 (7C, Ar), 123.0 (1C, Ar), 121.0 (1C, Ar), 111.2 (1C, Ar), 69.9 (1C, –CH$_2$OCH$_3$), 69.4 (1C, –CH$_2$OCH$_3$), 55.9 (1C, –NCH$_2$), 55.2 (1C, –NCH$_2$), 50.1 (1C, –NCH$_2$CH$_2$), 49.8 (1C, –NCH$_2$CH$_2$). ^{31}P NMR (80.98 MHz, CDCl$_3$) δ: 22.6. *Anal.* Calc. for C$_{26}$H$_{31}$ClNO$_3$PPdS$_2$: C, 48.60; H, 4.86; N, 2.18; S, 9.98. Found: C, 48.56; H, 4.83; N, 2.16; S, 10.01%.

5.2.5. [Pd(dimethyldithiocarbamate)(PPh$_2$Cl)Cl] (**5**)

Quantities used were 0.48 g (4.0 mmol) of dimethyldithiocarbamate and 2.47 g (4.0 mmol) of Pd(PPh$_2$Cl)$_2$Cl$_2$ in 25 mL of dichloromethane. Yield: 84% (0.17 g) of a golden yellow solid. M.p. 195–196 °C. FTIR (powder, cm^{-1}) 3053, 2962, 1534, 1433, 1096, 727, 689, 485, 383, 320. ^{1}H NMR (300 MHz, CDCl$_3$) δ: 7.73–7.66 (m, 6H, Ar*H*), 7.38–7.35 (m, 4H, Ar*H*), 3.25 (s, 3H, –NC*H*$_3$), 3.23 (s, 3H, –NC*H*$_3$). ^{13}C{^{1}H} NMR (75.47 MHz, CDCl$_3$) δ: 208.5 (1C, –*C*SS), 131.3 (2C, Ar), 131.0 (4C, Ar), 128.1 (6C, Ar), 39.1 (1C, –NCH$_3$), 39.0 (1C, –NCH$_3$). ^{31}P NMR (121.49 MHz, CDCl$_3$) δ: 84.0. *Anal.* Calc. for C$_{15}$H$_{16}$Cl$_2$NPPdS$_2$: C, 37.32; H, 3.34; N, 2.90; S, 13.29. Found: C, 37.00; H, 3.33; N, 2.91; S, 13.25%.

5.3. Structural studies

Crystals of complexes **1** and **2** were obtained by dissolving the product in a mixture of dichloromethane, *n*-hexane, and diethyl ether (2:1:1 v/v), and dichloromethane, *n*-hexane and petroleum ether (2:1:1 v/v), respectively. The solvents were slowly evaporated at room temperature in an open atmosphere and golden yellow crystals were obtained. The block crystals were mounted on a glass fibre using Paratone N hydrocarbon oil. The measurements were made at 200(2) K on a Bruker APEX II area detector diffractometer equipped with graphite monochromated Mo Kα radiation. The program used for retrieving cell parameters and data collection was APEX-2 [28]. The data were integrated using the program SAINT [29] and were corrected for Lorentz and polarization effects. The multiscan absorption corrections were performed using SADABS [30]. The structures were solved and refined using SHELXS-97 and SHELXL-97 (Sheldrick, 1997) [31] and all non-H atoms were refined anisotropically, with the hydrogen atoms placed at idealized positions.

5.4. Anti-tumor potato disc assay

For the assay of anti-tumour potato discs, the procedure of Mclaughlin et al. was followed [32]. *Agrobacterium tumefecien* (At 10) was grown for 48 h in lauria broth medium containing rifampicin (50 mg/ml). Red skinned potatoes were surface sterilized in a 0.1% mercuric chloride solution for 10 min and thoroughly washed with autoclaved distilled water. Potato discs (5 mm × 8 mm) were made with a borer and placed on agar (1.5%) plates (10 discs per plate). *Agrobacterium* cultures (600 μl) mixed with 150 μl each of 10,000, 1000, 100, 10, and 1 ppm of the compounds inoculum (in DMSO) were applied on the surface of each disc with the respective concentrations mentioned. The petri plates were then kept at 28 °C for 21 days. After 21 days, the discs were stained using Lugol's

solution (10% KI and 5% I_2) for 30 min and then observed under a dissecting microscope to calculate the number of tumors.

5.5. Cyclic voltammetric analysis

The cyclic voltammograms of the six complexes were performed in the absence and presence of DNA in CH_2Cl_2. The effect of scan rate was also studied and diffusion coefficients were calculated to estimate the heterogeneous rate constants. Voltammetric behavior of all the compounds was studied on a glassy carbon electrode at various scan rates (50–1000 mVs^{-1}). The Randles–Sevcik equation for an irreversible process was employed for the determination of the diffusion coefficient (D°) values [33]

$$I_p = (2.99 \times 10^5) n(\alpha n)^{1/2} AC(Dv)^{1/2} \quad (1)$$

where α is transfer coefficient, n is number of electrons transferred, A (cm^2) is area of working electrode, v (Vs^{-1}) is scan rate and C (mol/cm^3) is bulk concentration of the sample. αn was calculated from the equation reported in literature. $\alpha n = 47.7/(E_{pc} - E_{p/2})$ [34]. To calculate the standard heterogeneous rate constant, Gileadi's method was used [35]. From the shift in peak potential with the change in scan rate, the critical scan rate was determined, which was subsequently used in the following equation for the evaluation of k_{sh}

$$\log k_{sh} = -0.48\alpha + 0.52 + \log\left[\frac{\alpha n F v_c D^\circ}{2.3RT}\right] \quad (2)$$

To investigate the anti-tumor activity of the complexes, cyclic voltammetric measurements were made by varying the DNA concentration from 10 to 200 nM while keeping the concentration of the complex constant (5 mM). The complex-DNA binding constant was calculated according to the following equation [27]:

$$\log(1/[DNA]) = \log K + \log\{(I_{H-G})/(I_G - I_{H-G})\} \quad (3)$$

where, K is the binding constant, I_G and I_{H-G} are the peak currents of the free guest (G) and the complex (H–G), respectively.

Acknowledgements

Mr. Hizbullah Khan is highly grateful to the Higher Education Commission (HEC) of Pakistan for providing a scholarship under the programme "5000 Indigenous PhD Scholarships" at Quaid-i-Azam University Islamabad and six months scholarship under the "International Research Support Initiative programme (IRSIP)" as a Graduate Research Trainee, Department of Chemistry, Otto Maass Building, McGill University, Montreal, Quebec, Canada. F.-G. Fontaine would like to acknowledge CFI.

Appendix A. Supplementary material

Single crystal X-ray diffraction data for the structural analysis have been deposited with the Cambridge Crystallographic Data Centre, CCDC No. 813648 (**1**) and 813649 (**2**). Copies of this information may be obtained free of charge from the Director, CCDC, 12 Union Road, Cambridge, CB2 1EZ, UK (fax: +44 1223 336033; email: deposit@ccdc.cam.ac.uk or www:http://www.ccdc.cam.ac.uk).

References

[1] (a) H.M. Torshizi, M.I. Moghaddam, A. Divsalar, A.A. Saboury, J. Bioorg. Med. Chem. 16 (2008) 9616;
(b) B. Rosenberg, Cisplatin Chemistry and Biochemistry of a Leading Anticancer Drug, in: B. Lippert (Ed.), Verlag Chemie, VCH, 1999, p. 3.
[2] V. Alverdi, L. Giovagnini, C. Marzano, R. Seraglia, F. Bettio, S. Sitran, R. Graziani, D. Fregona, J. Inorg. Biochem. 98 (2004) 1117.
[3] M. Das, S.E. Livingstone, Br. J. Cancer 37 (1978) 466.
[4] V. Scarciaa, A. Furlania, D. Fregonab, G. Faragliab, S. Sitranc, Polyhedron 18 (1999) 2827.
[5] F.P.T. Hamers, C. Pette, B. Bravenenboer, Cancer Chemother. Pharmacol. 32 (1993) 162.
[6] I.E. Burgeson, N.M. Kostic, Inorg. Chem. 30 (1991) 4299.
[7] N. Farrell, Catalysis by Metal Complexes, Transition Metal Complexes as Drugs and Chemotherapeutic Agents, vol. 11, Kluwer Academic, Dordrecht, 1989. pp. 44–46.
[8] M.J. Cleare, J.D. Hoeshele, Platinum Met. Rev. 15 (1973) 42.
[9] G. Natile, M. Coluccia, Coord. Chem. Rev. 216–217 (2001) 383.
[10] S. Hidaka, M. Tsuruoka, T. Funakoshi, H. Shimada, M. Kiyozumi, S. Kojima, Ren. Fail. 16 (1994) 337.
[11] (a) D.L. Bodenner, P.C. Dedon, P.C. Keng, R. Borch, Cancer Res. 46 (1986) 2745;
(b) A. Trevisan, C. Marzano, P. Cristofori, M.B. Venturini, L. Giovagnini, D. Fregona, Arch. Toxicol. 76 (2002) 262.
[12] G. Durgaprasad, D.N. Sathyanarayana, C.C. Patel, Can. J. Chem. 47 (1969) 631.
[13] J.J. Criado, J.A.L. Aria, B. Marcias, L.R.F. Lago, Inorg. Chim. Acta 193 (1992) 229.
[14] M.M. Muir, J.A. Diaz, L.M. Torres, P. Nazario, Polyhedron 4 (1985) 155.
[15] F. Shaheen, A. Badshah, M. Gielen, G. Croce, U. Florke, D.D. Vos, S. Ali, Organomet. Chem. 695 (2010) 315.
[16] C. Paparizos, J.P. Fackler, Inorg. Chem. 19 (1980) 2886.
[17] F.H. Allen, O. Kennard, D.G. Watson, L. Brammer, A.G. Orpen, J. Chem. Soc., Perkin Trans. II (1987) S1.
[18] C.A. Tolman, Chem. Rev. 77 (1977) 313.
[19] (a) A.J. Downard, A.M. Bond, A.J. Clayton, L.R. Hanton, D.A. McMorran, Inorg. Chem. 35 (1996) 7684;
(b) K.C. Skyrianou, C.P. Raptopoulou, V. Psycharis, D.P. Kessissiglou, G. Psomas, Polyhedron 28 (2009) 3265;
(c) A.M. Bond, A.J. Canty, J.B. Cooper, C. Tedesco, P.R. Traill, D.M. Way, Inorg. Chem. Acta 251 (1996) 185.
[20] A.J. Bard, L.R. Faulkner, Electrochemical Methods: Fundamentals and Applications, second ed., Wiley, New York, 2001. p. 274.
[21] A.J. Bard, L.R. Faulkner, Electrochemical Methods: Fundamentals and Applications, Second ed., Wiley, New York, 2001. p. 239.
[22] Q.L. Zhang, J.G. Liu, H. Chao, G.Q. Xue, L.N. Ji, J. Inorg. Biochem. 83 (2001) 49.
[23] X. Jiang, X. Lin, Bioelectrochemistry 68 (2006) 206.
[24] A. Shah, R. Qureshi, N.K. Janjua, S. Haque, S. Ahmed, Anal. Sci. 24 (2008) 1437.
[25] A.J. Bard, L.R. Faulkner, Electrochemical Methods: Fundamentals and Applications, second ed., Wiley, New York, 2001. p. 501.
[26] M.S. Ibrahim, Anal. Chim. Acta 443 (2001) 63.
[27] M. Castillo, J.J. Criado, B. Marcias, M.V. Vaquero, Inorg. Chim. Acta 124 (1986) 127.
[28] Bruker (2005). APEX 2 Version 2.0.2. Bruker AXS Inc., Madison, Wisconsin, USA.
[29] Bruker (2003). SAINT Version 7.07a. Bruker AXS Inc., Madison, Wisconsin, USA.
[30] G.M. Sheldrick, SADABS Version 2004/1, Bruker AXS Inc., Madison, Wisconsin, USA, 2004.
[31] G.M. Sheldrick, SHELXS-97 and SHELXL-97, Programs for the refinement of crystal structures, University of Gottingen, Germany, 1997.
[32] J.L. Mclaughlin, L.L. Rogers, J.E. Anderson, Drug Info. J. 32 (1998) 513.
[33] J.E.B. Randles, Trans. Faraday Soc. 44 (1948) 327.
[34] A.J. Bard, L.R. Faulkner, Electrochemical Methods: Fundamentals and Applications, second ed., Wiley, New York, 2001. p. 236.
[35] E. Gileadi, V. Eisner, J. Electroanal. Chem. 28 (1970) 81.